

RECEIVED

MAR 25 1996

**CURRENT PROFILE MODIFICATION DURING LOWER HYBRID
CURRENT DRIVE IN THE PRINCETON BETA EXPERIMENT-
MODIFICATION***

R. Kaita, S. H. Batha,^a R. Bell, S. Bernabei, S. Hirshman,^b D. Ignat, S. Jardin, S. Jones,^c S. Kaye, J. Kesner,^c H. Kugel, B. LeBlanc, F. Levinton,^a S. Luckhardt,^d J. Manickam, M. Okabayashi, M. Ono, F. Paoletti,^e S. Paul, N. Sauthoff, S. Sesnic, H. Takahashi, W. Tighe, and S. von Goeler

DISCLAIMER

Plasma Physics Laboratory
Princeton University
Princeton, New Jersey 08543
USA

This report was prepared as an account of work sponsored by an agency of the United States Government. Neither the United States Government nor any agency thereof, nor any of their employees, makes any warranty, express or implied, or assumes any legal liability or responsibility for the accuracy, completeness, or usefulness of any information, apparatus, product, or process disclosed, or represents that its use would not infringe privately owned rights. Reference herein to any specific commercial product, process, or service by trade name, trademark, manufacturer, or otherwise does not necessarily constitute or imply its endorsement, recommendation, or favoring by the United States Government or any agency thereof. The views and opinions of authors expressed herein do not necessarily state or reflect those of the United States Government or any agency thereof.

ABSTRACT. Current profile modification with lower hybrid waves has been demonstrated in the Princeton Beta Experiment-Modification tokamak. When the $n_{||}$ spectrum of the launched waves was varied, local changes in the current profile were observed according to equilibria reconstructed from motional Stark effect polarimetry measurements. Changes in the central safety factor (q) were also determined to be a function of the applied radio frequency (rf) power. These results have been modeled with the Tokamak Simulation Code/Lower Hybrid Simulation Code, which is able to duplicate the general trends seen in the data.

MASTER

PACS: 52.30.Bt, 52.35.Fp, 52.35.Hr, 52.40.Db, 52.50.Gj, 52.70.Kz

1. INTRODUCTION

The ultimate attractiveness of the tokamak as a reactor concept is closely connected with the practicality of plasma control, especially the control of the plasma current profile. Lower hybrid current drive (LHCD) has been recognized as a promising technique for this purpose since its capability for substantial and sustained current drive was initially demonstrated.[1] Recent experiments on several tokamaks have continued to explore various issues related to future reactor applications.

LHCD experiments have been performed on ASDEX with rf powers up to 1.3 MW.² Changes in the internal inductance (ℓ_i) were clearly observed, and stabilization of sawtooth oscillations and $m=1$ modes was also achieved. Local measurements of the current density distribution, however, are not routinely available on ASDEX.[2] Enhanced confinement has been obtained with LHCD in Tore Supra.[3] Lower Hybrid Enhanced Performance (LHEP) plasmas were achieved at high toroidal field (4 T), where they exhibited a rapid rise in the central electron temperature (4.5 to 6-7 keV in 2 seconds), similar to the improved electron confinement observed in PLT.[4] Low toroidal field (<2 T) LHEP plasmas in Tore Supra had hollow current density profiles. These were deduced from q profiles obtained by Abel-inverting polarimetry measurements.

Studies of LHCD at high power have also been conducted recently on large tokamaks. The JT-60U team has compared normal LHCD with inverse current drive (i. e., against the plasma current) at the 3 MW level.[5] Changes in the current profile were determined from the different time evolutions of ℓ_i for the two cases.[5] A broadening of the current profile, as deduced from a reduction in ℓ_i , was also observed in LHCD experiments at 4 MW of rf power in JET.[6] External magnetic measurements were used to obtain the time evolution of the q profile in these discharges, and magnetic shear reversal was inferred over half of the plasma radius.[6] While all of these experiments provided important confirmation of current profile modification with LHCD, they did not include or had very limited local current profile measurements.

On the Princeton Beta Experiment-Modification (PBX-M), the effectiveness of LHCD in detailed modification of the plasma current distribution has been examined through measurements of the internal magnetic field with the multi-channel motional Stark effect (MSE) system.[7] It has a dedicated neutral probe beam (NPB)[8] that permits routine local current profile information without the perturbing effects of high-power neutral beam injection (NBI). The experimental safety factors presented in this paper are thus unique in that they are the only ones to date that are based on internal, local magnetic field data from plasmas with LHCD.

Measurements of LHCD efficiency as a function of the launched phase velocity and the dependence of the current profile modification on the applied rf power have been made using the MSE system. Equilibria for discharges without auxiliary heating, NBI only, and NBI combined with LHCD have also been reconstructed and compared as part of the development of scenarios for stable high poloidal beta (β_p) operation in PBX-M. The Tokamak Simulation Code/Lower Hybrid Simulation Code[9] has been used to model these cases, and the results exhibit the same parametric dependencies as the data.

2. EQUILIBRIUM RECONSTRUCTION

The practical application of MSE polarimetry for internal magnetic field measurements in tokamaks was first demonstrated in PBX-M.[7] A neutral hydrogen beam undergoes collisional excitation as it propagates through a plasma. The motion of the beam atoms across the confining magnetic field causes an electric field to be induced in their rest frame. A splitting in the wavelength of the emitted radiation results from this "motional Stark effect," and the emission transverse to magnetic field from the $\Delta m = \pm 1$ transitions is polarized parallel to the field. The polarization angle gives the direction of the magnetic field, and the spatial location of the measurement is determined from the intersection of the beam trajectory and the lines of sight of a multichannel spectrometer. The MSE diagnostic on PBX-M is a twelve-channel system with a spatial resolution of 3 cm.

The Variational Moments Equilibrium Code (VMEC)[10] has been utilized to perform equilibrium reconstructions using internal MSE magnetic field data as well as external flux loop measurements and plasma pressure distributions deduced from Thomson scattering profiles. The code first interpolates between MSE magnetic field pitch angle points and other discrete measurements with cubic spline fits, and uses the resulting continuous functions to solve the Grad-Shafranov equation. The details of VMEC are described elsewhere.[10] Evaluation of systematic and random errors suggest an uncertainty in the reconstructed equilibria of about 10%.[11]

3. CENTRAL SAFETY FACTOR MEASUREMENTS DURING LHCD

The dependence of central q on the phasing of the launched lower hybrid waves was studied in Ohmic plasmas, and the results are plotted in Fig. 1. The phasings ranged from 82.5 degrees to 120 degrees, which corresponded to $n_{||}$ values between 1.7 and 2.4. The data at a phasing of zero degrees reflect central q values measured in the absence of LHCD. The convention used in this paper is that phasings given in positive degrees refer to wave propagation in the same direction (“co-direction”) as the plasma current. The applied rf power was between 210 kW and 289 kW. The NPB injection time was varied from shot to shot to obtain MSE data at different times during the interval when rf power was applied. Even so, the scatter in the $q(0)$ values for plasmas without LHCD (zero phasing) fell within 10% of the mean value of 0.8.

Higher lower hybrid power appears to be needed to affect $q(0)$, as shown in Fig. 2. Since the lower hybrid wave damping and the resulting current drive efficiency are functions of plasma density, it was used to normalize the lower hybrid power. The data are also divided by the major radius to allow comparison with other devices, so the units of the abscissa are 10^{15} kW cm².

The MSE measurements in deuterium plasmas (circles) all occurred at the same time in the discharge. The $q(0)$ values for discharges with and without LHCD were within 10% of a mean value of

0.85, except for one point at the very highest normalized rf power. The hydrogen data were obtained under two different sets of plasma conditions. The triangles are the $q(0)$ values from plasmas without NBI. The squares refer to plasmas that included rf power from 307 to 391 kW, and NBI between 530 and 560 kW.

For the hydrogen plasmas, the greater change in $q(0)$ occurs at higher rf power. The discharges with the three highest $q(0)$ values had both NBI and LHCD, and the central electron density was about 8% higher than in the cases where NBI was absent. This makes the change in $q(0)$ in Fig. 2 appear more dramatic for a modest increase in normalized rf power.

The conditions for the deuterium and hydrogen plasmas with NBI are summarized in Table I. The $q(0)$ values for the representative cases with LHCD correspond to the same launched phasing (90°) and similar normalized rf power ($\approx 40 \times 10^{15}$ kW cm²). The reason for the difference in the $q(0)$ values achieved with LHCD in hydrogen and deuterium plasmas is not clear. The density and rf power ranges for these discharges overlap, and they all exhibit sawtooth oscillations in the absence of LHCD. In addition, the most significant increase in $q(0)$ for hydrogen discharges occurred at NBI and LHCD power levels well within the range covered by the deuterium data. The modeling of these plasmas with a lower hybrid ray tracing code (Section 5) indicates that the wave damping is not a sensitive function of plasma species.

The larger change in $q(0)$ in hydrogen plasmas may be related to the current distribution in the Ohmic target plasma. The internal inductance (ℓ_i) is lower for the hydrogen discharges compared to the deuterium shots (Fig. 3). This is consistent with a deuterium current density that is initially more peaked, as seen in the comparison of representative deuterium and hydrogen profiles without LHCD in Fig. 4. Although it is not clear why the latter tend to be less peaked, it may be easier to flatten a current distribution that is already broad with the same amount of off-axis current drive. These results thus suggest that the starting current distribution may in fact be a significant factor that governs the efficiency of LHCD in current profile modification.

4. HIGH β_p SCENARIO WITH NBI AND LHCD

A stable operational path to high β_p was found by first increasing $q(0)$ with off-axis LHCD in an Ohmic discharge, and then heating the plasma with NBI. The results are described in this section. MSE measurements were obtained for the initial Ohmic plasma, the phase with LHCD alone, and combined LHCD and NBI. The VMEC equilibria constrained with MSE measurements were reconstructed in each of these cases, and the $q(0)$ values were included in the power scan data described in the preceding section. The MSE pitch angle data and VMEC fit for an $I_p = 180$ kA Ohmic hydrogen plasma is shown in Fig. 5, and it represents a $q(0)$ of 0.93. This value of $q(0)$ is consistent with the presence of sawtooth oscillations.

With the addition of 300 kW of LHCD, emission profiles from a soft X-ray diode array show a steady decrease in magnetohydrodynamic (MHD) activity (Fig. 6). The 32 diodes in the array integrate the soft X-ray emission along chords in a poloidal cross section of the plasma, and the z-axis corresponds to their intersection with a line normal to the plasma center. The contours reflect high X-ray intensities that occur during precursors to sawteeth oscillations, and their steady shrinkage toward $z=0$ suggests that the $q=1$ surface similarly decreases with time. About 200 ms after the start of LHCD, the sawtooth oscillations and $m/n=1/1$ modes were suppressed and $q(0)$ was raised to 1.15. After 175 msec of NBI at the 530 kW level, β_p doubled from 0.5 to 1.0. The discharge remained quiescent to MHD activity, however, and the central q stayed above 1 ($q(0) = 1.1$).

To determine if beam-driven currents themselves could maintain $q(0)$ above 1, we compared discharges having NBI alone with plasmas where LHCD and NBI were combined. The corresponding current density profiles are shown in Fig. 7, and the q profiles are compared in Fig. 8. A measure of the shape of the current distribution is the ratio of the central current density to its value near the mid-minor radius point, $j(0)/j(r = 15 \text{ cm})$. This was 2.2 for the Ohmic plasma and 2.4 for discharges with NBI only. With both NBI and LHCD, however, the ratio falls to 1.4, which reflects a profile that is clearly broader

and shows more off-axis current than in the NBI only case. The central q was 0.87 for the plasma with NBI only, and sawtooth oscillations were present as in the Ohmic discharge. In all of these cases (Ohmic, NBI only, and NBI combined with LHCD), the plasma current was 180 kA and the toroidal field was 13.5 kG.

5. MODELING WITH SIMULATION CODES

The Tokamak Simulation Code[12] combined with the Lower Hybrid Simulation Code⁹ (TSC/LSC) has been applied to the parameters of the high- β_p plasmas. The program assumes an axisymmetric toroidal geometry, and it uses ray tracing to determine the lower hybrid wave propagation. The TSC/LSC model was used to study wave absorption and current drive efficiency in earlier PBX-M[9] and Tokamak de Varennes[13] experiments, and the predictions were generally in good agreement with the data. In these earlier cases, however, detailed comparisons between the measured and model q profiles were not performed.

The high- β PBX-M experiments with LHCD described in the preceding section were in the regime of multipass absorption at low electron temperature and high density. In the original TSC/LSC model, this led to an extreme and unphysical localization of the wave damping, which was governed by the maximum parallel index of refraction permissible for these plasmas.[14,15] From the highly peaked rf-driven current that resulted, the code predicted a shear reversal in the q profile (Fig. 9) and a significant off-axis current that was not seen in the data. The code actually failed at 380 ms, when the calculated $q(0)$ far exceeded the maximum measured value and approached 1.5.

To correct this problem, a heuristic mechanism for diffusing the non-inductive current was added to the code.[16] A current smoothing consistent with a diffusion coefficient of $1 \text{ m}^2/\text{s}$ was assumed. This value falls within the range ($0.5 - 2 \text{ m}^2/\text{s}$) deduced from hard X-ray camera imaging of superthermal electron transport during LHCD.[17] The rf power-deposition profile should also reflect this smoothing, so the code broadens it according to a weighting scheme that uses the density and the diffused non-

inductive current distribution.[16]

The reversed shear in the q profile and the strong edge peaking of the current profile were eliminated. This is demonstrated in Fig. 10, which shows the model q profile as it evolves over 100 ms beyond the point where the calculation without the diffusion model terminated. In this case, the calculated $q(0)$ reaches a value slightly above 1.2, which is within the experimental uncertainty. The model q profile remains monotonic with time, as in the data, and a reversed shear region never develops.

The results of the modeling with a diffusion coefficient of $1 \text{ m}^2/\text{s}$ are compared with the data in Table II. The values are comparable for hydrogen but differ for deuterium, where the $q(0)$ from experiment is significantly lower than in hydrogen under similar conditions. The ray tracing and transport should not depend strongly on plasma species, and the similarity in the $q(0)$ values computed with TSC/LSC for the two cases supports this. To help resolve the discrepancy, more measurements in hydrogen are needed and planned over the full range of normalized rf power achieved in deuterium plasmas.

7. SUMMARY

The internal magnetic field measurements during LHCD with the MSE diagnostic on PBX-M are unique in their extensiveness. In particular, they have demonstrated the dependence of current profile modification on the rf power applied to the plasma. These results indicate that the current profile can be controlled with even modest levels of LHCD. With measurements of q profiles that were modified with LHCD and maintained during NBI, experiments on PBX-M have demonstrated a scenario for achieving high β_p through off-axis current drive and beam heating.

The $q(0)$ values achieved with LHCD in hydrogen and deuterium plasmas, at the same density and rf power, are not the same. The current distribution in Ohmic hydrogen target plasmas tend to be less peaked, and so it may be easier to flatten a current distribution that is already broad with the same

amount of off-axis current drive. This implies that the initial current distribution may determine the efficiency of LHCD in current profile modification.

The internal magnetic field measurements were also sufficiently accurate to test the LHCD assumptions in the TSC/LSC model. Measurements of the energetic electron distribution during LHCD showed that the radial diffusion of the superthermal electrons was small but still finite. A consequence of this is a broadening of the rf power deposition profile and a diffusion of the rf current.

A comparison of the TSC/LSC calculations with the MSE profiles show the importance of including these effects in predicting the basic features of current profile modification in PBX-M. The best agreement between the data and the modeling is obtained with current smoothing based on a diffusion coefficient of $1 \text{ m}^2/\text{s}$. This value is consistent with observations of superthermal electron transport using a hard X-ray camera to image plasmas with LHCD.

*Work supported by U.S.D.O.E. Contract DE-AC02-76-CH03073

^aFusion Physics and Technology, Inc., Torrance, California USA

^bOak Ridge National Laboratory, Oak Ridge, Tennessee USA

^cMassachusetts Institute of Technology, Cambridge, Massachusetts USA

^dUniversity of California at San Diego, San Diego, California USA

^eCentre d'Études Nucleaires, Grenoble, FRANCE

REFERENCES

- [1] BERNABEI, S., et al., Phys. Rev. Lett. **49**, 1255 (1982).
- [2] SOLDNER, F. X., et al., Nucl. Fusion **34**, 985 (1994).
- [3] EQUIPE TORE SUPRA, to be published in the Proceedings of the Eleventh Topical Conference on Radio Frequency Power in Plasmas, Palm Springs, CA (1995).
- [4] BELL, R., et al., Phys. Rev. Lett. **60**, 1294 (1988).

- [5] MORI, M. and the JT-60 TEAM, Plasma Phys. Cont. Fusion **36 (12B)**, B181 (1994).
- [6] THE JET TEAM, TO Be published in the Proceedings of the Fifteenth International Conference on Plasma Physics and Controlled Nuclear Fusion Research, Seville, Spain (1994).
- [7] LEVINTON, F. M., et al., Phys. Rev. Lett. **63**, 2060 (1989).
- [8] KUGEL, H. W., et al., Nucl. Instrum. and Methods **B40/41**, 988 (1989).
- [9] IGNAT, D., et al., Nucl. Fusion **34**, 837 (1994).
- [10] HIRSHMAN, S. P., et al., Phys. Plasmas **1**, 2277 (1994).
- [11] LEVINTON, F., et al., Phys. Fluids B **5**, 2554 (1993).
- [12] JARDIN, S. C., et al., J. Comp. Phys. **66**, 481 (1986).
- [13] DEMERS, Y., et al., to be published in the Proceedings of the Eleventh Topical Conference on Radio Frequency Power in Plasmas, Palm Springs, CA (1995).
- [14] TAKAHASHI, H., Phys. Plasmas **1**, 2254 (1994).
- [15] PAOLETTI, F., et al., Nucl. Fusion **34**, 771 (1994).
- [16] IGNAT, D., et al., (in press).
- [17] JONES, S., et al., Plasma Phys. Control. Fusion **35**, 1003 (1993).

FIGURE CAPTIONS

1. Central q as a function of launched lower hybrid wave phasing in Ohmic hydrogen plasmas.
2. Central safety factor as a function of rf power normalized to density and major radius for hydrogen and deuterium plasmas. The units for the abscissa are 1015 kW cm^2 .
3. Internal inductance as a function of central q in plasmas with hydrogen (open squares) and deuterium (closed squares) as the working gas.
4. Comparison of current profiles for representative Ohmic plasmas with deuterium (solid line) and hydrogen (dashed line) as the working gas. The values for the internal inductance (ℓ_i) are given

for each discharge.

5. MSE data and VMEC fit for Ohmic plasma.
6. Contour plot showing time evolution of soft X-ray emission along sightlines in poloidal cross section of PBX-M plasma.
7. Comparison of measured current density profiles with NBI only (solid line) and combined NBI and LHCD (dashed line).
8. Comparison of measured safety factor (q) profiles with NBI only (solid line) and combined NBI and LHCD (dashed line).
9. Time evolution of q profile from TSC/LSC for LH+NBI without diffusion model.
10. Time evolution of q profile from TSC/LSC for LH+NBI as in Fig. 9, but with model assuming diffusion coefficient of 1 m²/s.

	$n_e(0)$ (10^{13} cm ⁻³)	RF Power (kW)	NBI Power (kW)	$\langle q(0) \rangle$ (no LHCD)	$q(0)$ (w/LHCD)
Deuterium	2.7-4.3	180-434	280-630	0.85 ± 0.1	0.90 ± 0.1
Hydrogen	3.0-5.4	307-391	530-560	0.93 ± 0.1	1.15 ± 0.1

Table I. Summary of $q(0)$ values obtained in deuterium and hydrogen plasmas.

	Hydrogen ($\approx 40 \times 10^{15}$ kW cm ²)	Deuterium ($\approx 40 \times 10^{15}$ kW cm ²)
$q(0)$ from experiment	1.15 ± 0.1	0.90 ± 0.1
$q(0)$ from TSC/LSC	1.22	1.22

Table II. Comparison of experimental values of $q(0)$ with calculations using TSC/LSC assuming a diffusion coefficient of 1 m²/s.

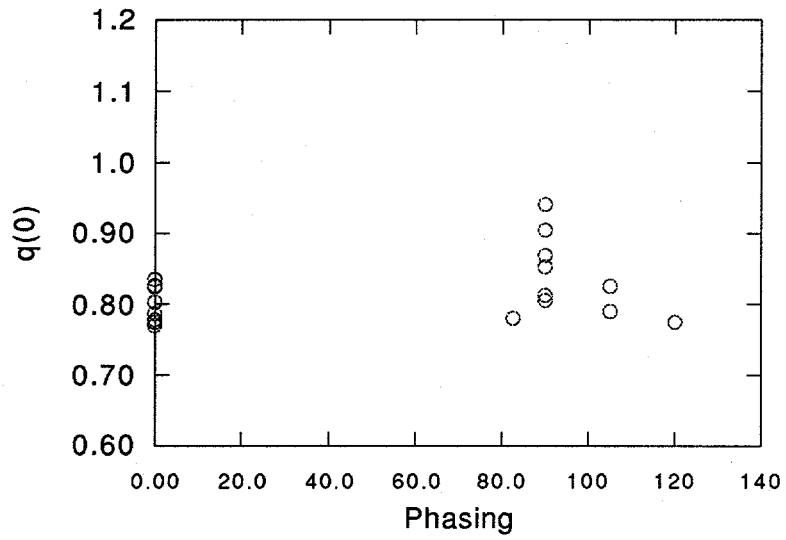


Fig. 1

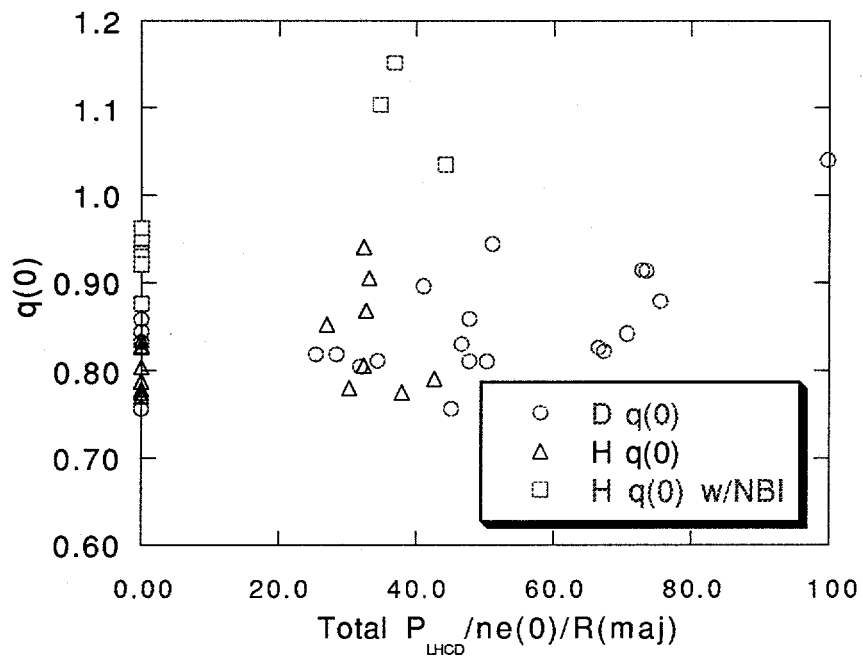


Fig. 2

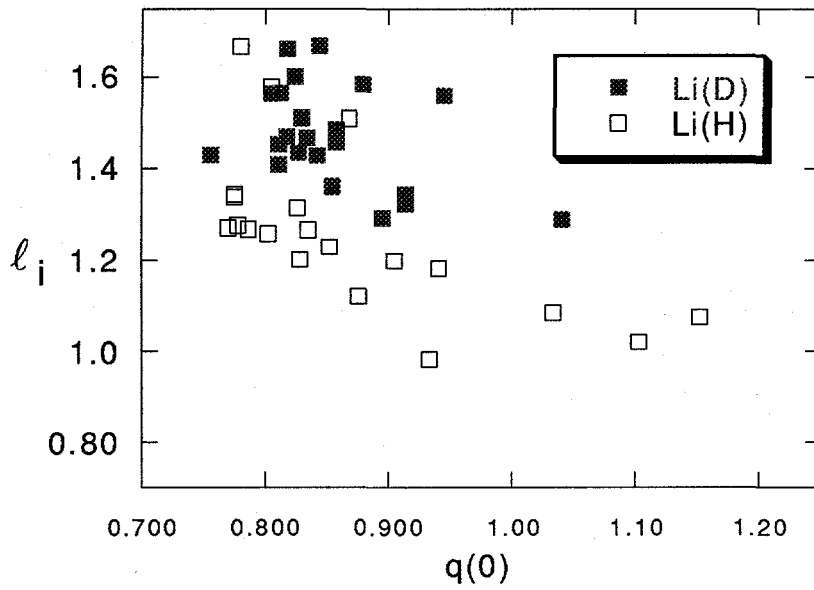


Fig. 3

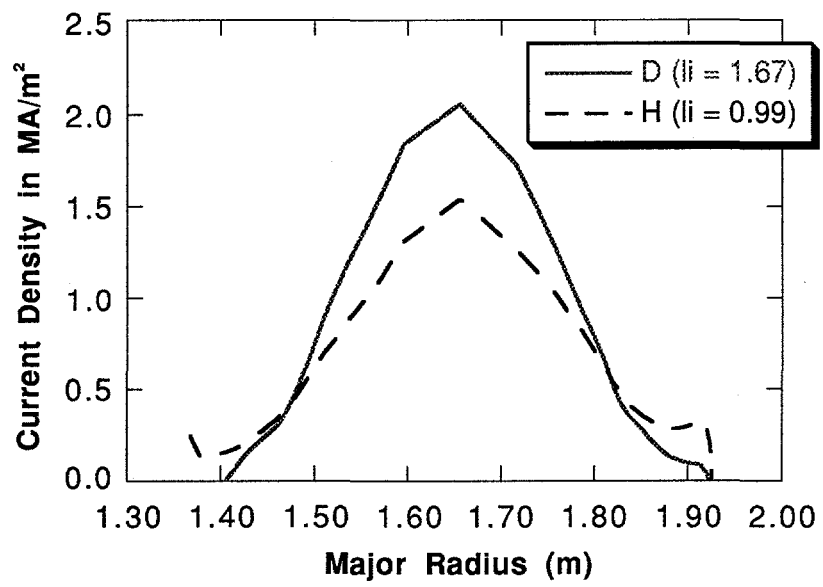


Fig. 4

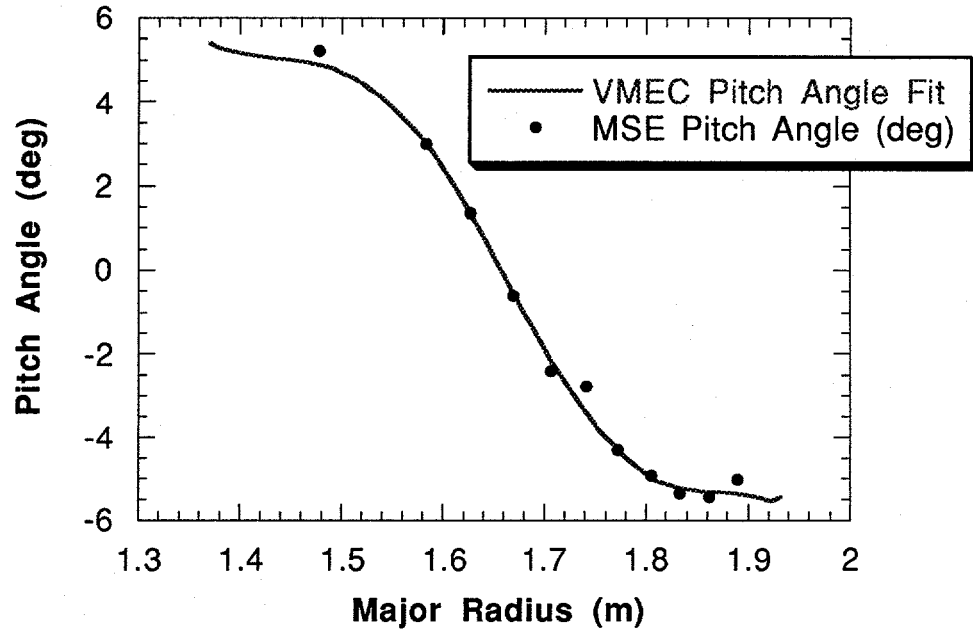


Fig. 5

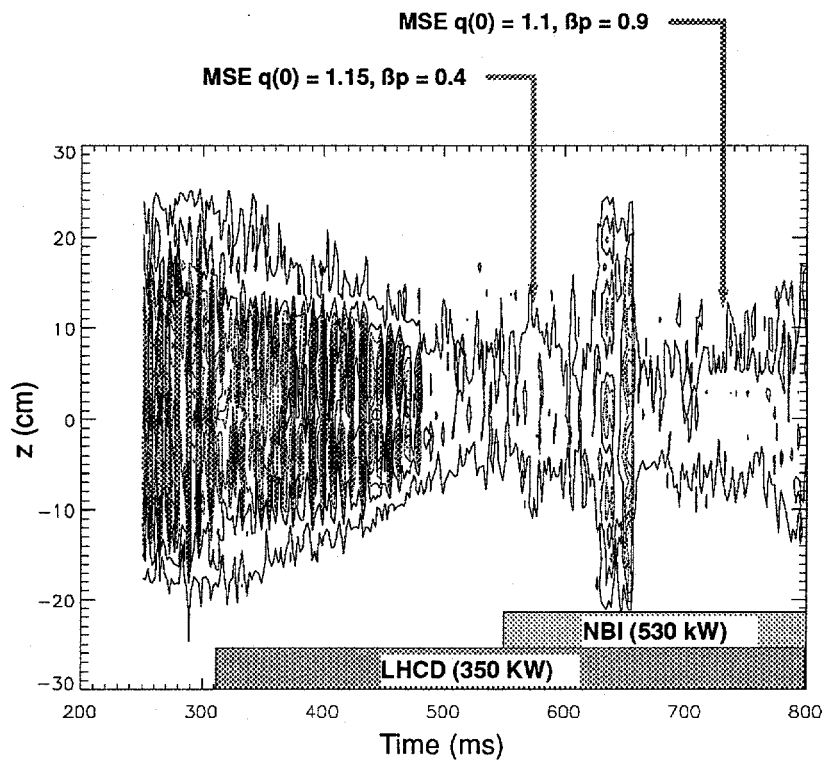


Fig 6

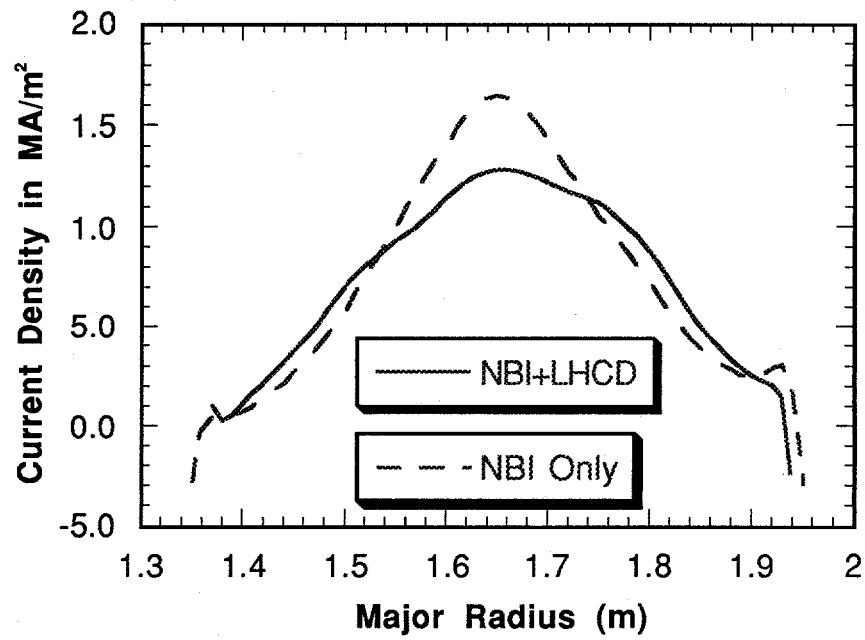


Fig. 7

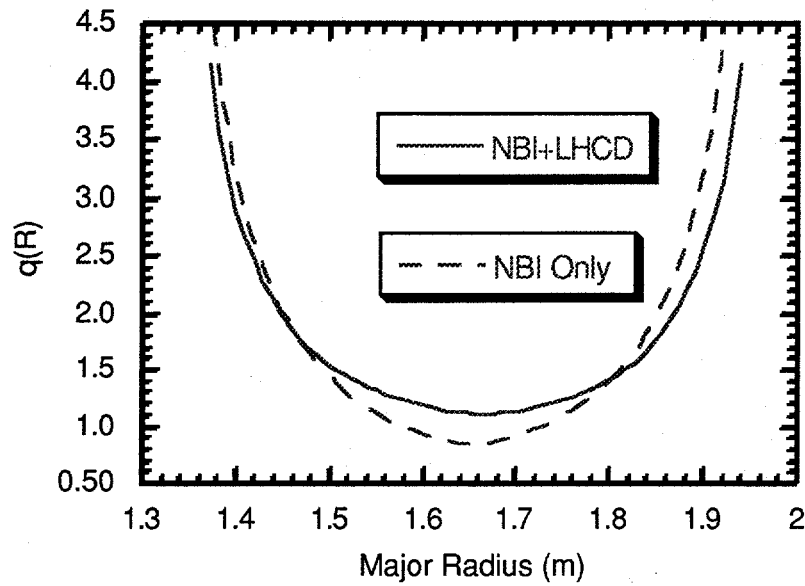


Fig. 8

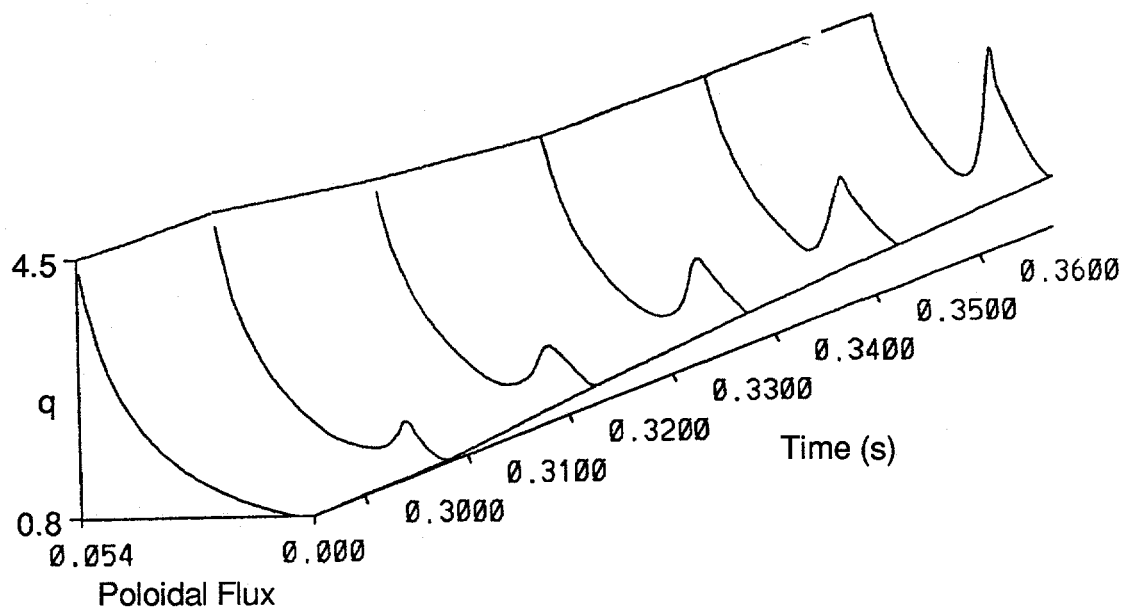


Fig 9

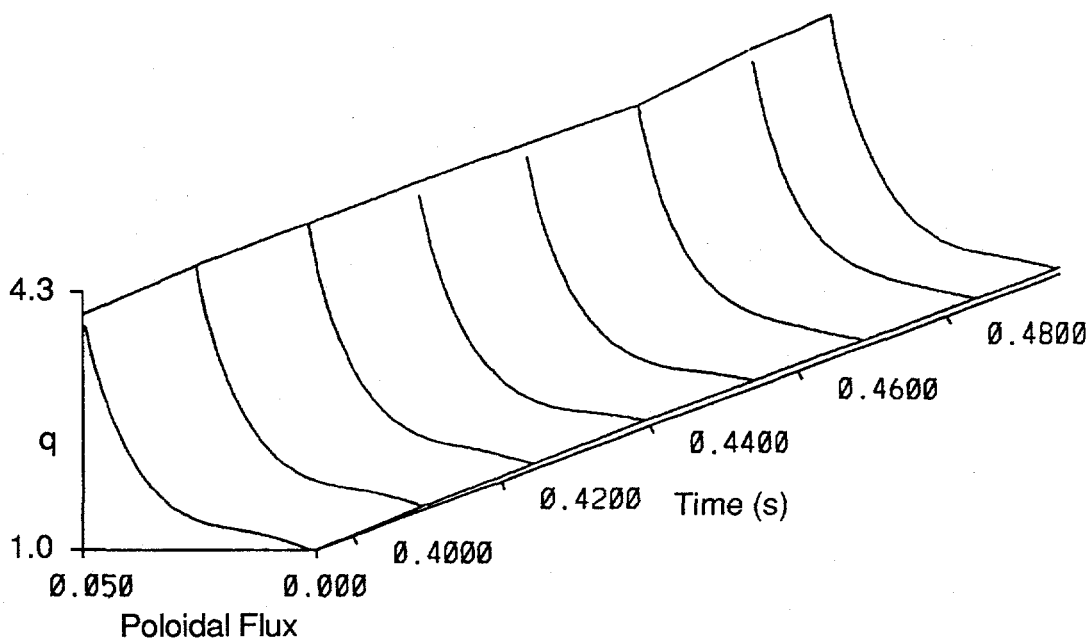


Fig 10